Dependence of ZnO Nanostructured Thin Films Properties on Growth Temperature by APCVD Method

M. Maleki[a],[*] and S.M. Rozati[b]

[a]Department of Physics, Faculty of Science, Fouman and Shaft Branch, Islamic Azad University, Fouman, Iran
[b]CVD Lab., Physics Department, University of Guilan, Namjoo St., Faculty of Science, Rasht, Iran

In this paper, the effect of substrate temperature on the electrical, structural, morphological and optical properties of nanostructured polycrystalline zinc oxide thin films were investigated by the Hall measurement, X-ray diffraction, scanning electron microscopy and UV-visible spectrophotometer, respectively. Then these modified thin films were deposited on two kinds of single crystal and polycrystalline of n- and p-type Si in three different substrate temperatures of 300, 400 and 500 °C by low cost atmospheric pressure chemical vapor deposition method. Like the samples grown on the glass substrate, with increase of the temperature in samples grown on single crystal Si, preferred orientation changes from (100) to (002), while in samples deposited on poly crystalline Si, preferred orientation remains (100).

1. Introduction

ZnO is an n-type II–VI group compound with a wurtzite structure. ZnO films have been widely studied owing to their usefulness in electronic or optoelectronic applications, gas sensors, solar cell windows, and surface acoustic-wave devices [1–4].

Based on many reviewed articles from 1985 up to now, there are many articles in which they investigated doped ZnO in order to obtain the best TCO layers for solar cell applications [5–12]. The best resistivity was reported in the range of 3.4×10^{-3} Ω cm for ZnO:Al [7] to about 10^{-5} Ω cm for ZnO:In [5], while the transparency of the layers changed in the range 80–90%. Although these results are praiseworthy, there are few articles about pure ZnO and the effect of substrate temperature on electrical, optical, structural and morphological properties "simultaneously" with low cost atmospheric pressure chemical vapor deposition (APCVD) method.

For example, in 1999, Haga et al. produced conductive transparent ZnO films with the best resistivity of about 10^{-2} Ω cm and the transparency of about 80% [13]. They studied the effect of ozone generation rate on electrical properties of ZnO layers. In 2000, Takahashi et al. studied the effect of substrate temperature on growth rate of ZnO films with the precursors of $ZnCl_2$ and O_2 [14]. Their research was devoted to structural properties and FWHM changes with O_2 and $ZnCl_2$ pressure. In 2002, Fu et al. investigated the structure and photoluminescence (PL) at room temperature of ZnO films deposited on Si (111) substrates by metal-organic chemical vapor deposition (MOCVD) using diethylzinc (DEZ) and CO [15]. It was found that these properties strongly depend on growth temperature and pressure.

Morphological and structural properties of ZnO thin films were studied by Hong et al. in 2003 [16]. They used single source chemical vapor deposition (SSCVD) under low vacuum conditions with the precursor of zinc carbamate $Zn_4O(CO_2Net_2)_6$. Careful quantitative XPS analysis revealed that the ZnO films were stoichiometric with O/Zn atomic ratio very close to that of ZnO single crystal. In 2005, Kopalko et al. reported that monocrystalline films were obtained only for GaN/Al_2O_3 substrates, whereas use of sapphire, silicon or soda lime glass resulted in either 3D growth mode or in polycrystalline films showing preferential orientation along the c axis [17]. In 2006, Romero et al. studied the effect of kind of precursor on structural properties of ZnO thin films [18]. They concluded that the preferred orientation can be altered by changing the deposition conditions: the substrate temperature, the precursor solution composition or by introducing aluminum. In 2007, growth of ZnO films and nanowires (NWs) by atmospheric pressure chemical vapor deposition (APCVD) using Zn powder and water as source materials were performed [19].

Photoluminescence intensity ratio of the green band at about 2.5 eV to the near-band-edge emission at about 3.2 eV decreased with increase of the source feeding ratio of H_2O to Zn (VI/II), indicating the possibility of the defect control. In 2008, ZnO thin films were prepared using zinc chloride, zinc acetate and zinc nitrate precursors by spray pyrolysis technique on glass substrates at 550 °C [20]. Regardless of precursors, ZnO thin films were all in hexagonal crystallographic phase and had (002) preferred orientation. Scanning electron microscopy (SEM) images showed completely different surface morphologies for each precursor in ZnO thin films. ZnO rod was observed only for zinc chloride precursor. The optical measurements revealed that films had a low transmittance and a direct band gap approximately 3.30 eV. In 2009, ZnO thin films synthesized by chemical bath deposition were used as buffer layer

_____

[*]corresponding author; e-mail: m.maleki@fshiau.ac.ir

between the anode and the organic electron donor in organic solar cells [21]. In 2010, ZnO thin films were grown on glass substrate by APCVD, using zinc acetate as precursor of Zn and ozone as an oxidant agent [22]. The structural and optical properties of ZnO films were investigated in different deposition temperatures (300–375 °C in steps of 25 °C). All deposited films were polycrystalline in (100) preferred orientation and had transparency of about 80% in the visible region. In 2011, zinc oxide thin films were deposited on glass substrates from room temperature to 673 K by using DC magnetron sputtering [23]. The preferred orientation for ZnO thin films lies along (002) direction and the average crystallite size was determined from the Scherrer formula. SEM images showed that grain sizes of zinc oxide thin films was found to be in the range of 15–28 nm.

In 2012, it was shown that variations in the ratio of oxygen to zinc precursors at constant temperature allow changing the surface morphology of zinc oxide (ZnO) films deposited by low pressure MOCVD, while keeping the sheet resistance and transparency of the layers constant [24].

In 2014, boron doped zinc oxide films were prepared at different water to diethyl zinc ratios by a low pressure CVD technique [25]. It was found that the morphology of the films vary from small leaf like to pyramidal surface structures with increase of H_2O/DEZ flow ratio.

Therefore, in this paper we want to investigate the effect of deposition temperature on electrical, optical, structural and morphological properties of pure ZnO thin films by the Hall effect and Van der Pauw setup, UV-visible spectrophotometer, X-ray diffractometer and SEM measurement. Also, in order to study the importance of the kind of the substrate on modifying structural properties, we used two types of Si substrate.

2. Experimental techniques

2.1. Sample preparation

The glass substrates were degreased as described in our previous work [26]. We have used oxygen gas with purification of 99.999 (contained: maximally 2 ppm argon, 5 ppm nitrogen, 0.5 ppm hydrogen, 0.5 ppm $CO + CO_2$, 0.5 ppm methane + hydrocarbons and 1 ppm water) and zinc acetate ($C_4H_6O_4Zn\cdot2H_2O$) as precursors. The mass of zinc acetate was 0.2 g in all experiments and we introduced it as powder directly in the reactor with a distance about 5 cm from the substrate. Deposition was carried out in a homemade APCVD described in our previous study [27]. Oxygen flow rate was kept at 200 °C/min, substrate temperature was changed in the range 300–500 °C and layers were deposited during 1 h.

ZnO films were deposited onto silicon substrates in an open tube system by the oxidation of $C_4H_6O_4Zn\cdot2H_2O$. Before deposition, the silicon substrates were degreased about 2 min in solution of hydro fluoric acid and deionised water then rinsed in deionised water. These silicones were cleaned ultrasonically in acetone and rinsed

again in deionised water. The cleaned Si substrates were introduced in the tubular furnace. The thickness of two types of Si were 650 and 750 μm; their resistivity were 3.51×10^2 Ω cm, 4.95×10^2 Ω cm; their mobility were 207, 822 ($cm^2/(V\ s)$) and their carrier concentration were 2.44×10^{14}, 4.63×10^{12} cm^{-3} for polycrystalline and single crystal Si, respectively. Polycrystalline Si was p-type with B doped, while single crystal Si was n-type with P doped. Single crystal silicon's orientation is (400). Our samples were grown at an oxygen flow rate of 200 sccm in substrate temperature of 300, 400 and 500 °C during 1 h.

2.2. Sample characterization

The electrical properties of thin films were measured by the Hall effect and Van der Pauw setup (RH 2010 — PhysTech system). A UV-visible spectrophotometer (Cary 100 Scan Varian) was employed for obtaining transmittance spectra. A spectrophotometric transmittance graph of the film was used for the thickness calculation by the Swanepoel method [28]. The crystalline structure was obtained by means of an X-ray diffractometer with Cu K_α radiation (Philips-pw-1830). The morphology of the surface of films was examined by scanning electron microscopy (EM-3200,KYKY).

3. Results and discussion

3.1. Electrical properties

Figure 1 shows changes of sheet resistance versus deposition temperature. With increase of substrate temperature from 300 °C, sheet resistance increases and after a maximum at 450 °C it decreases. For more investigation, from Fig. 2, which presents changes of electrical parameters such as resistivity, carrier concentration and mobility versus deposition temperature, it can be deduced that this figure is in accordance with sheet resistance diagram.
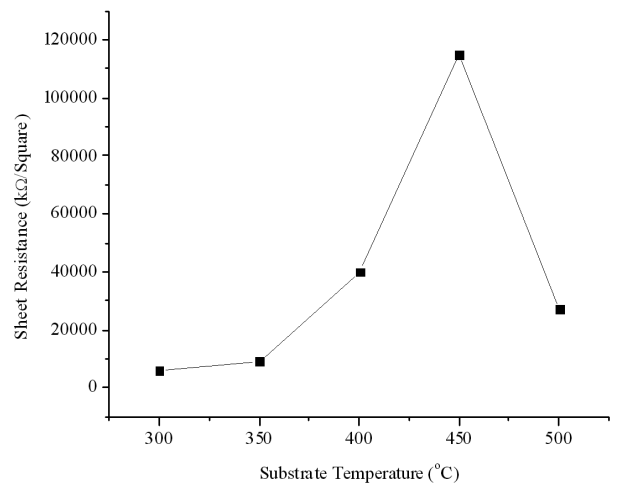
Fig. 1. Changes of sheet resistance versus deposition temperature.

As shown in Fig. 2, with increase of substrate temperature, resistivity increases and after reaching a
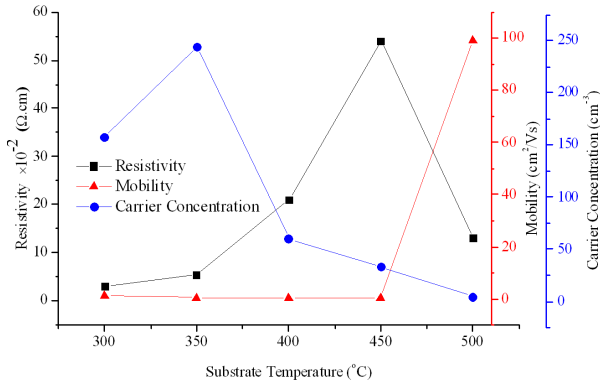
Fig. 2. Changes of electrical parameters such as resistivity, carrier concentration and mobility versus deposition temperature.

maximum, it decreases. While mobility does not show clear change up to 450 °C and with more increase of substrate temperature, it suddenly increases severely. We can relate this suddenly increase of mobility with decrease of carrier concentration scattering as a result of carrier decreasing. Also, mobility improves due to grain size increase which will be discussed in the following. As a result of this suddenly increase of mobility, resistivity decreases. With respect to the diagram, it is clear that carrier concentration decreases with increasing temperature. It is reasoned that when the substrate temperature is increased, the number of oxygen atoms adsorbed on the thin films will be increased, causing a decrease of the defect density and resulting in a decrease of the carrier concentration [29]. These results imply that as the substrate temperature is increased from 300 to 450 °C, the thin films come closer to the stoichiometrical composition. Our results are in good agreement with Kang et al. report in which they used pulsed laser deposition method with different precursors [30].

TABLE

Values of electrical parameters of the samples for various substrate temperatures. Type of doping — n (for all temperatures).

Temperature [°C]	Thickness [nm]	Sheet resistance [$\Omega/\square$]	Resistivity [Ωcm]	Hall co. [cm^3/A s]	Mobility [cm^2/V s]	Carrier concentration [cm^{-3}]	Type
300	508	6.14×10^6	3.12×10^2	-3.96×10^2	1.27	1.57×10^{16}	n
350	608	8.98×10^6	5.46×10^2	-2.56×10^2	0.5	2.44×10^{16}	n
400	526	3.99×10^7	2.1×10^3	-1.4×10^3	0.5	5.98×10^{15}	n
450	474	1.15×10^8	5.47×10^3	-1.88×10^3	0.3	3.32×10^{15}	n
500	487	2.71×10^7	1.32×10^3	-1.32×10^3	99	4.74×10^{14}	n

Table shows changes of thickness, sheet resistance, resistivity, Hall coefficient, mobility, carrier concentration and the type of carrier versus deposition temperature.

3.2. Structural and morphological properties

Figure 3 shows typical XRD patterns of the ZnO layers grown on glass substrate at different deposition temperature. All films have polycrystalline structure with a hexagonal wurtzite structure. Although the peaks intensity is so weak at low deposition temperature, with increase of temperature it increases. This is due to the low atomic mobility, which constrains the growth of the crystal during the crystallization process at low temperatures. As the substrate temperature increases up to 500 °C, enough thermal energy is supplied to the adatoms on the substrate and increases the surface mobility leading to an increase in the (002) plane orientation [30].

At substrate temperature of 300 and 400 °C, preferred orientation is (100) while at 500 °C it changes to (002). The primary effect of a change in composition from an oxygen-deficient material to stoichiometric ZnO is a preferred (002) orientation [31, 32]. With increasing substrate temperature, ZnO layers approach to a stoichiometric ones and preferred orientation changes to (002) peak.

Since amount of the oxygen incorporation into lattices may increase at higher substrate temperature [33]. Also, the thermal energy of the substrate can supply enough energy necessary to form the (002) orientation. As a result, the films prepared at the higher temperature show a good crystalline quality [33].

As depicted in Fig. 4, the increase of grain size as a result of temperature increase is clear. The mean crystallite size D was calculated for the diffraction peaks using the Scherrer formula [34]. Grain size was calculated for (002) orientation. This demonstrated that the crystallinity of ZnO films was likely to improve with increase of deposition temperature. Although some others used different precursors and other deposition methods, our results are in good agreement with theirs [10, 35].

Figure 5 shows typical XRD patterns of the ZnO layers grown on single and polycrystalline Si at three substrate temperatures of 300, 400 and 500 °C. It is worth noticing this fact that samples which have been grown at all substrate temperatures have polycrystalline structure. Like
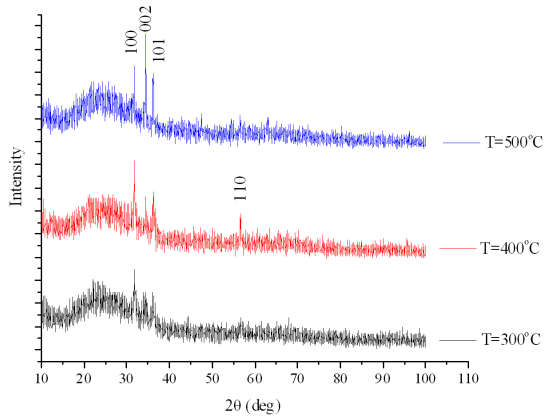
Fig. 3.   XRD patterns of the ZnO layers grown on glass substrate at different deposition temperature.
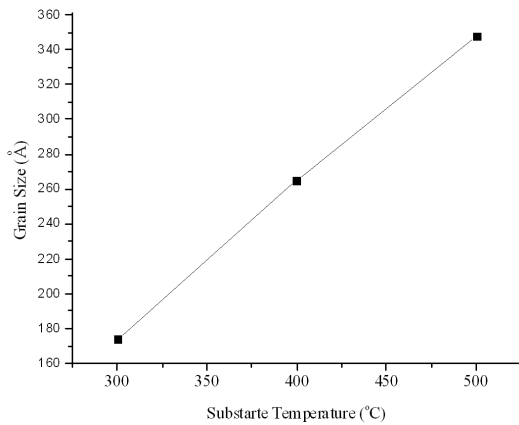
Fig. 4.   Changes of grain size as a result of temperature increase.
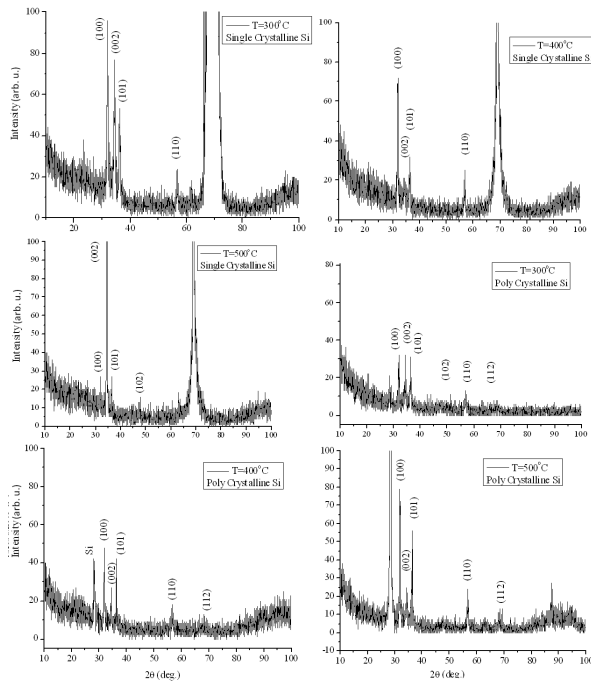
Fig. 5.   XRD patterns of the ZnO layers grown on single and polycrystalline Si at three substrate temperatures of 300, 400 and 500 °C.

the samples grown on the glass substrate, with increase of the temperature in samples grown on single crystal Si, preferred orientation changes from (100) to (002), while in samples deposited on poly crystalline Si, preferred orientation remains (100). The surface energy of the (002) orientation takes minimum in the ZnO crystal, and then in order to grow a *c*-axis oriented ZnO crystal, it is important that the particles ablated from the target have still energy at the substrate surface [33]. It seems that in the case of ZnO layers on polycrystalline Si, particles do not have enough energy to form ZnO layers with (002) preferred orientation. We can relate this phenomenon to the type of the polycrystalline Si. Indeed, (100) preferred orientation in this case can be formed due to the presence of the residual stress in the film that depends on experimental conditions and substrate nature.

As expected in both cases, with increasing temperature, the intensity of the preferred peak increases due to improving crystallinity. The effect of Si substrate is clear with its peak at about 70° for single crystal Si and at 28° for polycrystalline Si.
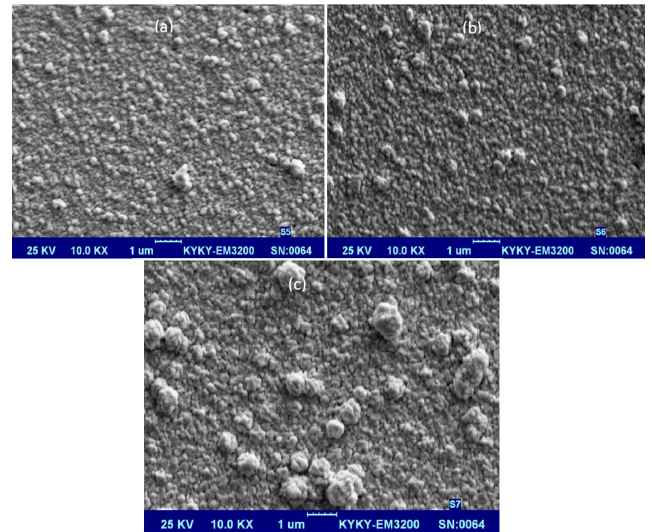
Fig. 6.   SEM images of the ZnO thin films deposited at various glass substrate temperatures.

Figure 6 shows SEM images of the ZnO thin films deposited at various glass substrate temperatures. All of the thin films show nanometer-sized grains and a dense microstructure. In the case of the thin films deposited at 300 °C, small grains were observed. As the substrate temperature is increased up to 500 °C, the surface morphology is observed to consist of larger and more packed grains.

3.3. Optical properties

Figure 7 shows transmission spectra of ZnO thin films at different substrate temperatures. All layers have acceptable transmission for solar cell applications. As it is clear, transparency does not have distinct change due to low carrier concentration of the samples. As a result,

absorption of free carrier concentration is low and transparency is high. These results are in accordance with Fay et al. report [36].
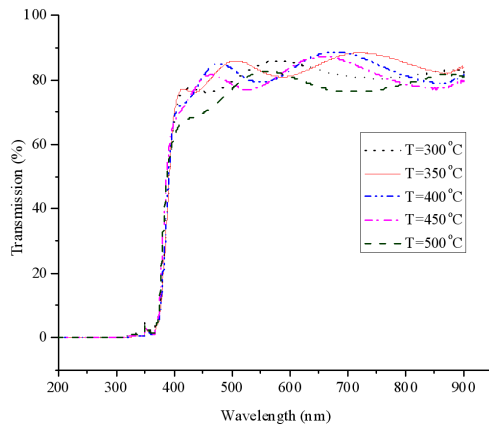
Fig. 7. Transmission spectra of ZnO thin films at different substrate temperatures.
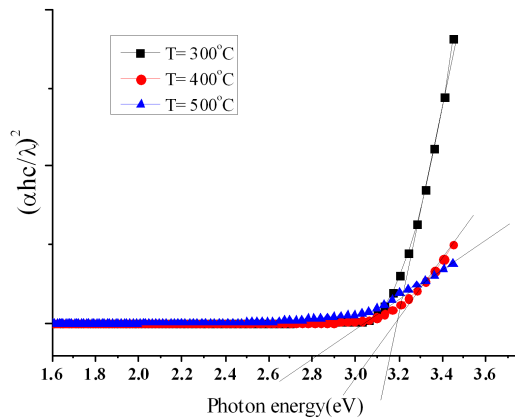
Fig. 8. Optical band gap of ZnO thin films at substrate temperature of 300, 400, 500 °C.

The optical band gap, E_g of the ZnO thin films was determined by extrapolation of the linear portion of $(\alpha h\nu)^2$ versus $h\nu$ plots by applying the Tauc model which is clear in Fig. 8 [37].

As the growth temperature was reduced from 500 to 300 °C, the optical band gap blueshifted from 2.8 to 3.2 eV. A similar blueshift phenomenon of optical band gap was also observed in ZnO thin films deposited on quartz substrate [38]. Decrease of band gap as a result of increase of substrate temperature can be explained by the composition variation as a function of the growth temperature [39].

4. Conclusions

According to this paper, we studied the effect of deposition temperature on optoelectrical, structural and morphological properties of ZnO thin films. From the Hall measurement, resistivity increased with substrate temperature, as a result of increase of the number of oxygen atoms adsorbed on the thin films, causing a decrease of the defect density and resulting in a decrease of the carrier concentration. In accordance with electrical properties, structural properties of both layers grown on glass substrate and Si substrate improved due to deposition temperature increase and these results were approved by SEM images. As the substrate temperature increased enough thermal energy was supplied to the adatoms on the substrate and increased the surface mobility leading to an increase in the (002) plane orientation. Also, as a result of increasing crystallinity, transparency improved. Finally, transparency and band gap was acceptable for thin film ZnO while electrical properties should be modified by other factors such as doping, etc.

References

[1] M. Pacio, H. Juarez, G. Escalante, G. Garcia, T. Diaz, E. Rosendo, *Mater. Sci. Eng. B* **174**, 38 (2010).

[2] P. Nunes, E. Fortunato, R. Martins, *Mater. Res. Soc. Symp. Proc.* **666**, 1 (2001).

[3] A.A. Ibrahim, A. Ashour, *J. Mater. Sci. Mater. Electron.* **17**, 835 (2006).

[4] S. Wu, R. Ro, Z.X. Lin, *Appl. Phys. Lett.* **94**, 1 (2009).

[5] S. Major, A. Banerjee, K.L. Chopra, *Thin Solid Film* **125**, 179 (1985).

[6] J. Hu, R.G. Gordon, *Solar Cells* **30**, 437 (1991).

[7] T. Minami, H. Sato, H. Sonohara, S. Takata, T. Miyata, I. Fukuda, *Thin Solid Films* **253**, 14 (1994).

[8] B.M. Ataev, A.M. Bagamadova, V.V. Mamedov, A.K. Omaev, *Mater. Sci. Eng. B* **65**, 159 (1999).

[9] B.K. Meyer, J. Sann, D.M. Hofmann, C. Neumann, A. Zeuner, *Semicond. Sci. Technol.* **20**, S62 (2005).

[10] S.M. Park, T. Ikegami, K. Ebihara, *Thin Solid Films* **513**, 90 (2006).

[11] J.G. Lu, T. Kawaharamura, H. Nishinaka, Y. Kamada, T. Ohshima, S. Fujita, *J. Cryst. Growth* **299**, 1 (2007).

[12] C.F. Yu, S.H. Chen, S.J. Sun, H. Chou, *J. Phys. D Appl. Phys.* **42**, 035001 (2009).

[13] K. Haga, F. Katahira, H. Watanabe, *Thin Solid Films* **343**–**344**, 145 (1999).

[14] N. Takahashi, K. Kaiya, K. Omichi, T. Nakamura, S. Okamoto, H. Yamamoto, *J. Cryst. Growth* **209**, 822 (2000).

[15] Z. Fu, B. Lin, J. Zu, *Thin Solid Films* **402**, 302 (2002).

[16] D. Hong, B. Gong, A.J. Petrella, J.J. Russell, R.N. Lamb, *Sci. China (Series E)* **46**, 355 (2003).

[17] K. Kopalko, A. Wójcik, M. Godlewski, E. Łusakowska, W. Paszkowicz, J.Z. Domagała, M.M. Godlewski, A. Szczerbakow, K. Świątek, K. Dybko, *Phys. Status Solidi C* **2**, 1125 (2005).

[18] R. Romero, D. Leinen, E.A. Dalchiele, J.R. Ramos-Barrado, F. Martin, *Thin Solid Films* **515**, 1942 (2006).

[19] T. Terasako, M. Yagi, M. Ishizaki, Y. Senda, H. Matsuura, S. Shirakata, *Thin Solid Films* **516**, 159 (2007).

[20] E. Bacaksiz, M. Parlak, M. Tomakin, A. Ozcelik, M. Karakız, M. Altunbas, *J. Alloys Comp.* **466**, 447 (2008).

[21] Y. Lare, A. Godoy, L. Cattin, K. Jondo, T. Abachi, F.R. Diaz, M. Morsli, K. Napo, M.A. del Valle, J.C. Bernede, *Appl. Surf. Sci.* **255**, 6615 (2009).

[22] M. Pacio, H. Juarez, G. Escalante, G. Garcia, T. Diaz, E. Rosendo, *Mater. Sci. Eng. B* **174**, 38 (2010).

[23] B. Rajesh Kumar, T. Subba Rao, *Digest J. Nanomater. Biostruct.* **6**, 1281 (2011).

[24] S. Nicolay, M. Benkhaira, L. Ding, J. Escarre, G. Bugnon, F. Meillaud, C. Ballif, *Solar Energy Mater. Solar Cells* **105**, 46 (2012).

[25] M. Wan, H. Zhu, Y. Wang, J. Yin, J. Gao, Z. Wang, F. Gun, Y. Mai, Y. Huang, W. Yu, S. Huang, *Appl. Phys. A* **115**, 297 (2014).

[26] M. Maleki, S.M. Rozati, *Phys. Scr.* **86**, 015801 (2012).

[27] M. Maleki, S.M. Rozati, *Bull. Mater. Sci.* **36**, 217 (2013).

[28] R. Swanepoel, *J. Phys. E Sci. Instrum.* **16**, 1214 (1983).

[29] N. Srinivasa Murty, S.R. Jawalekar, *Thin Solid Films* **102**, 283 (1983).

[30] S.J. Kang, Y.H. Joung, H.H. Shin, Y.S. Yoon, *J. Mater. Sci. Mater. Electron.* **19**, 1073 (2008).

[31] K.H. Yoon, J.W. Choi, D.H. Lee, *Thin Solid Films* **302**, 116 (1997).

[32] M.J. Brett, R.R. Parsons, *J. Mater. Sci.* **22**, 3611 (1987).

[33] T. Ohshima, R.K. Thareja, T. Ikegami, K. Ebihara, *Surf. Coat. Technol.* **169–170**, 517 (2003).

[34] B.D. Cullity, *Elements of X-Ray Diffraction*, Addison-Wesley, Reading 1978.

[35] G. Luka, T. Krajewski, L. Wachnicki, B. Witkowski, E. Lusakowska, W. Paszkowicz, E. Guziewicz, M. Godlewski, *Phys. Status Solidi A* **207**, 1568 (2010).

[36] S. Fay, U. Kroll, C. Bucher, E. Vallat-Sauvain, A. Shah, *Solar Energy Mater. Solar Cells* **86**, 385 (2005).

[37] J. Tauc, *Amorphous and Liquid Semiconductors*, Plenum, London 1974.

[38] S.T. Tan, B.J. Chen, X.W. Sun, H.S. Kwok, W.J. Fan, X.H. Zhang, S.J. Chua, *J. Appl. Phys.* **98**, 013505 (2005).

[39] G. Sanon, R. Rup, A. Masingh, *Phys. Rev. B* **44**, 5672 (1988).